J Musculoskelet Neuronal Interact 2014; 14(4):401-410

Original Article

Hylonome

Peripheral quantitative computed tomography-derived muscle density and peripheral magnetic resonance imaging-derived muscle adiposity: precision and associations with fragility fractures in women

A.K.O. Wong[1,2], K.A. Beattie[2], K.K.H. Min[2], C. Gordon[3], L. Pickard[2,4], A. Papaioannou[4], J.D. Adachi[2] & the Canadian Multicentre Osteoporosis Study (CaMos) Research Group

[1]Osteoporosis Program, University Health Network, Toronto, ON; [2]Department of Medicine, McMaster University, Hamilton, ON; [3]Department of Nuclear Medicine, McMaster University, Hamilton, ON; [4]Hamilton Health Sciences, Hamilton, ON, Canada

Abstract

Purpose: To determine the degree to which muscle density and fractures are explained by inter and intramuscular fat (IMF). **Methods:** Women ≥50 years of age (Hamilton, ON, Canada) had peripheral magnetic resonance imaging and peripheral quantitative computed tomography scans at 66% of the tibial length. Muscle on computed tomography images was segmented from subcutaneous fat and bone using fixed thresholds, computing muscle density. IMF was segmented from muscle within magnetic resonance images using a region-growing algorithm, computing IMF volume. Fracture history over the last 14 years was obtained. Odds ratios for fractures were determined for muscle density, adjusting for IMF volume, total hip BMD, age and body mass index. **Results:** Women with a history of fractures were older (N=32, age:75.6±8.3 years) than those without (N=39, age: 67.0±5.2 years) (<0.01). IMF volume explained 49.3% of variance in muscle density (p<0.001). Odds for fractures were associated with lower muscle density even after adjusting for IMF volume but were attenuated after adjusting for age. **Conclusions:** Muscle adiposity represents only 50% of the muscle density measurement. Properties of muscle beyond its adiposity may be related to fractures, but larger and prospective studies are needed to confirm these associations.

Keywords: peripheral Quantitative Computed Tomography (pQCT), peripheral MRI, Inter- and Intramuscular Fat, Muscle Density, Fragility Fractures

Introduction

Muscle contracts on bone, imparting microstrains that are sensed by bone's osteocytes, which respond by altering bone remodeling[1]. The muscle-bone relationship has been demonstrated by a number of investigators, all observing a positive relationship between muscle mass or area and indices of bone strength[2-4]. Muscle, bone and fat all derive from mesenchymal stem cells and there may be factors that result in a preferential shift from one cell type to another[5-7]. When there is a preferential commitment towards adipocytes, the consequence may be a loss of bone or muscle. This phenomenon may be more evident with aging[8]. Given these two potential mechanisms for the observed relationship between muscle and bone strength, there is motivation for exploring the direct association between muscle or muscle adiposity and fragility fractures.

Muscle contains more mass per unit volume than fat. The density of entire muscle groups, known crudely as muscle density (MD), can serve as a proxy for the amount of fat infiltration into and between muscle groups[9]. However, this measure of density also reflects the compactness of muscle fibres, the amount of protein within muscle and other potential soft-tissue

Andy Kin On Wong, Karen A. Beattie, Kevin K.H. Min, Christopher L. Gordon, Laura Pickard, Alexandra Papaioannou, and Jonathan D. Adachi declare that they have no conflicts of interest.

Corresponding author: Andy K.O. Wong, Toronto General Research Institute, University Health Network, 200 Elizabeth St, Eaton 7th floor 7EB-238, Toronto, ON, M5G 2C4, Canada
E-mail: andy.wong@uhnresearch.ca

Edited by: F. Rauch
Accepted 5 December 2014

elements not segmented from muscle such as tendons, blood vessels, aponeuroses and fascia. Using QCT, McDermott et al showed that smaller leg MD increased the risk for mobility loss (HR=3.50(1.28,9.57)) in 370 men and women ≥59 years old[10], supporting the functional relevance of MD. Tinetti and Laroche also highlighted the importance of leg muscles for the avoidance of a fall: a large determinant in the development of a fracture[11,12]. Goodpaster showed that a significant relationship between thigh and mid-leg MD exists (r=0.60)[9]. Using pQCT, leg MD can be quantified but it remains unknown to what extent MD actually reflects the amount of fat between and within muscle groups, versus other soft tissue components. Magnetic resonance imaging (MRI) can provide high-contrast images displaying clear distinctions between muscle and both inter- and intra (I)-muscular (M) fat (F), the sum of both fat compartments hereon forward referred to as IMF. In older adults, Ruan demonstrated using MRI that a single slice of the leg muscles measuring intermuscular adipose tissue represented up to 58% of total body adipose tissue and 52% of total body intermuscular adipose tissue[13]. Despite the more crude measurement of MD achievable by single-slice CT, Goodpaster validated MD against muscle lipid content (R^2=18-33%)[9]. However, MD has not been validated *in vivo*.

To date, only one study by Sheu et al has demonstrated a direct relation between intermuscular fat of the abdominal muscles derived from fixed-threshold segmentation of QCT images and incident non-spine fractures[14]. Muscle density, the proxy for adiposity, has been previously associated with fractures[15]. However, it is possible that non-fat-related components of muscle may be responsible for this association. The present study therefore aimed to determine the association between MD and MRI-derived IMF, to quantify the relationship between fragility fractures and each of MD and IMF, and to explore what proportion of the relationship between MD and fractures can be explained by differences in IMF. It is hypothesized that IMF explains more than 30% of MD and that a larger amount of muscle adiposity reflected by larger IMF and lower MD is associated with a higher risk of fractures. It is also anticipated that MD is no longer associated with fractures after accounting for direct measurements of IMF.

Methods

This investigation was designed as a cross-sectional observational study examining the relationship between pQCT and MRI muscle measurements obtained in the present and pre-existing fragility fractures that have occurred within the 14 years prior to these muscle measurements. All study procedures were performed in a cohort (Hamilton, ON, Canada) representing an intended population of peri- and post-menopausal Canadian women. All muscle measurements were collected within 1.5 years. Women ≥50 years of age enrolled in the Canadian Multicentre Osteoporosis Study (CaMOS) and living within a 50 km radius of the Hamilton CaMOS site were considered eligible to participate (N=340) in this study. The CaMOS study is an ongoing, prospective cohort study of community-dwelling, randomly selected women and men ≥25 years of age at nine major Canadian cities. The main CaMOS objectives, methodology and sampling framework are described in detail elsewhere[16]. Participants were randomly selected from eligible women by research staff to yield this pilot sample. Women with contraindications to MR imaging (pacemaker, insulin pumps) or weighing above 250 lbs were excluded from 1.0T peripheral(p)MRI procedures due to the weight limit of the positioning chair.

Participants volunteered in the completion of a pQCT and 1.0 T pMRI leg scan at the largest cross-section of the leg represented by the 66% site of the tibia length as measured from the distal articulating aspect of the medial malleolus towards the medial articulating aspect of the tibial plateau. In a subset of individuals, both scans were repeated once after complete removal from the scanner within the same visit to assess short-term test-retest reproducibility of MD and IMF measurements. These individuals were asked to return a year later to complete a repeat scan on both pQCT and pMRI to obtain long-term precision of MD and IMF measurements. A complete list of current medications including dose, duration and frequency was collected at study visit. Information on medical conditions and ascertained incident fragility fractures from the last 14 years was obtained from the CaMOS database[16]. The most recently available total hip areal bone mineral density (aBMD) (within 1-3 years) through the CaMOS database was also obtained. Fragility fractures were defined as non-traumatic fractures occurring as the result of a fall from standing height or less, excluding any fractures of the skull, fingers and toes. All study procedures were overseen and approved by the St. Joseph's Healthcare Research Ethics Board in Hamilton.

Peripheral quantitative computed tomography

A single 2.5±0.3 mm thick slice was acquired at the 66% region of interest as indicated by a line drawn on the leg, with an in-plane resolution of 500 μm, a CT scan speed of 15 mm/s, 38 kVp X-ray beam energy, a tube current of 0.3 mA, reconstructed by filtered back-projection on a matrix size of 256 x 256 (Figure 1). Hydroxyapatite phantoms were assessed on days in which scans were obtained. Only images with no discontinuities in the cortical bone were accepted for image analyses.

Automatic threshold-based iterative edge-detection-guided segmentation of muscle from bone was performed using a density threshold of 280 mg/cm^3 with contour mode 1 and peel mode 2 (bone area and mass). Segmentation of muscle from subcutaneous fat followed a threshold of 40 mg/cm^3 with contour mode 3 and peel mode 1 (total muscle+bone area and mass) after applying a smoothing filter (F03F05). All threshold-based segmentations were performed using Stratec Analysis Software v6.0 (Orthometrix Inc., White Plains, NY, USA) by a single image analyst who was blinded to fracture status and demographics of participants. To determine muscle cross-sectional area (MCSA), bone area was subtracted from total bone + muscle area. Similarly, bone mass was subtracted from total bone + muscle mass to derive muscle mass. Muscle den-

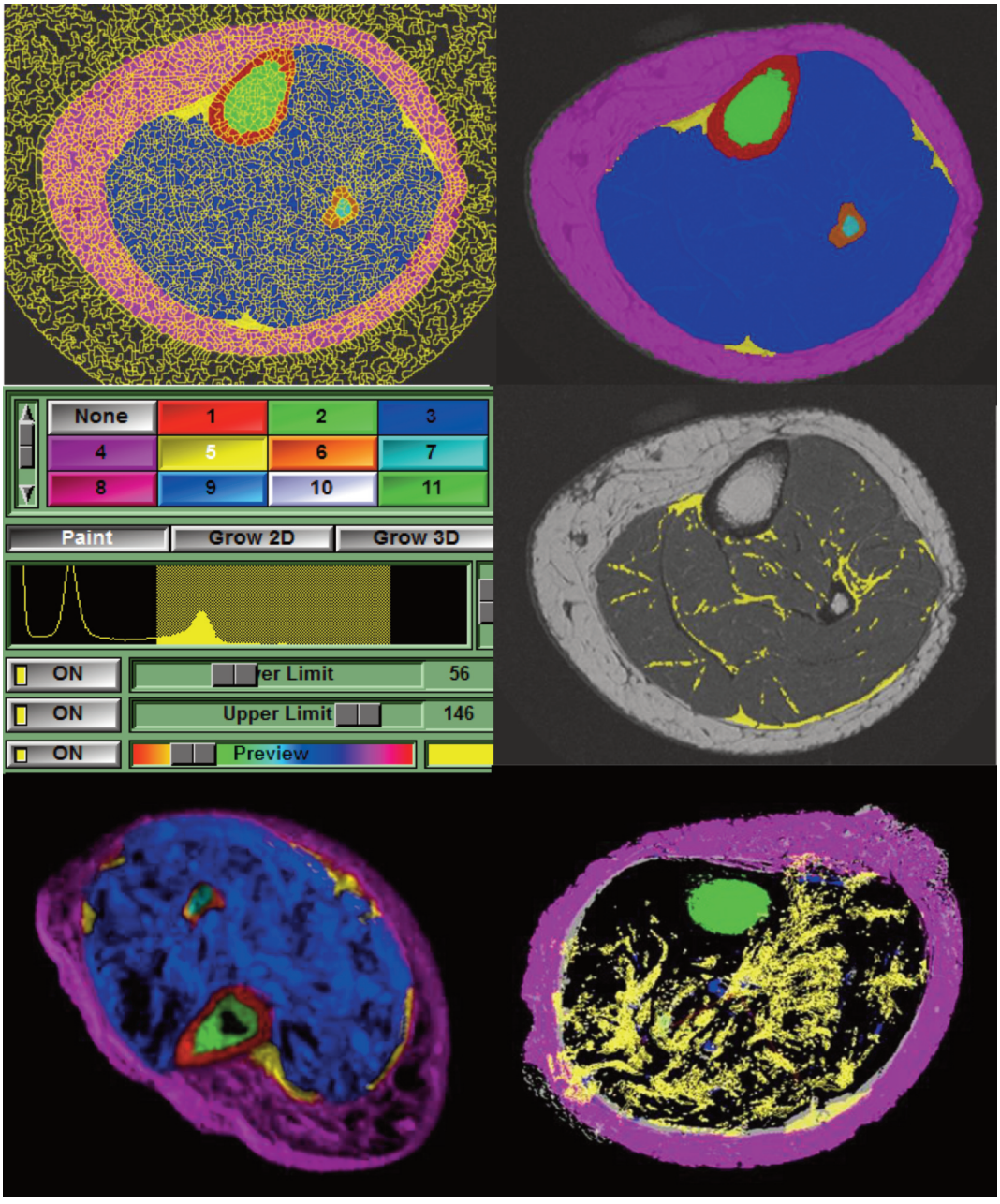

Figure 1. Watershed and region growing algorithm-guided muscle and fat segmentation. Top row: illustration of the watershed lines generated for enabling manual segmentation of muscle from subcutaneous fat. Middle row: threshold setting for region-growing algorithm guiding IMF segmentation. Bottom row: 3D rendering of the 10 MRI slices. Yellow = IMF (inter and intra-muscular adiposity). Pink = subcutaneous fat. Green = tibial bone marrow fat. Light blue = fibular bone marrow fat. Red = tibial cortical bone. Orange = fibular cortical bone.

sity was computed by dividing total muscle mass by MCSA. Because scans were not routinely performed with an air-water-bone phantom, Hounsfield unit calibration was not available. To better express meaningful values, units were retained in mg/cm^3 based on a calibration using a hydroxyapatite-equivalent European forearm phantom. For reference, the linear attenuation coefficient (LAC) could be back calculated using the following equation: LAC= (MD+322.06) / 1724.41).

1.0 Tesla peripheral magnetic resonance imaging

Leg scans were also performed on a 1.0T pMRI OrthOne scanner (GE Healthcare, USA) using a 180 mm diameter transmit/receive coil. A series of fiducial markers were placed at the 66% site line. The largest cross-section of the leg muscles was positioned in the iso-centre of the bore of the magnet while the participant was seated in a chair on wheels. On the coronal scout view, a reference line was placed at the 66% site

fiducial markers. All slices were aligned perpendicular to the long axis of the tibia. Ten slices were prescribed and centred so that the middle slices were located at the reference line. A T1-weighted fast spin echo sequence was acquired transaxially with the following sequence parameters: TR/TE: 600/21 ms, NEX=3, echoes=2, flip angle=40°, bandwidth=25 kHz, yielding ten 1.0 mm thick contiguous slices at 500 μm in-plane resolution (Figure 1). A geometric phantom was assessed on days in which scans were obtained. Only images that exhibited no breaks in the cortical bone of the tibia were accepted for image analyses. SliceOmatic 4.3 (TomoVision, Montreal, QC, Canada) was used to complete all MR image segmentations.

The watershed algorithm available on SliceOmatic was used to segment muscle from subcutaneous fat by a separate image analyst blinded to the fracture status and demographics of participants, including the results of pQCT muscle segmentation. Water-shed lines were configured with thresholds set at 1 pixel surface and a 0.01% mean difference, yielding a fine mesh of water-shed pools (Figure 1 top row). Muscle, subcutaneous fat, cortical bone and marrow regions were filled while ignoring all IMF fat deposits. Next, a threshold-guided region-growing algorithm was used to segment IMF from within the muscle area. No distinction between inter- and intramuscular compartments of fat within the muscle fascia line was made during segmentation. A signal intensity histogram guided the selection of upper and lower thresholds to define IMF areas. Because each participant's MR image exhibited a slightly different signal intensity histogram, a consistent threshold cannot be applied to all images. Instead, the image analyst used the base of the fat peak as a guide, and used visual inspection to fine-tune a consistent level of fat to segment (Figure 1 middle row). All image segmentations were performed on the same computer screen with gamma settings fixed upon each sitting. The central 5 slices were segmented and summated to generate total muscle and IMF volumes (IMF.V) (Figure 1 bottom row). The central most slice was used to compute single-slice IMF surface area (IMF.A) for a sensitivity analysis. Fat volume or area was divided by muscle plus fat volume or area, multiplied by 100% to give percent IMF.V or IMF.A, respectively.

Physical function tests

To capture other aspects of muscle not addressed by the imaging outcomes, physical function tests were performed. The timed 'up-and-go' (TUG) test evaluated lower leg strength, coordination and mobility using the original protocol by Podsiadlo et al[17] on a standard chair with arms. Hand grip strength was measured using the Jamar 200 lb hand dynamometer (Austin, TX, USA) following a validated protocol previously described[18]. The grip strength of both arms was measured over three trials and the maximum measurement was used.

Data analyses

An analysis of variance followed by a least significant difference post-hoc test determined whether there were significant differences in anthropometrics, medication use, physical function and muscle imaging outcomes between those with and without a history of fragility fractures. Root mean square coefficients of variation (RMSCV) and standard deviations (RMSSD) were computed to determine the short-term and one-year test-retest precision error for pQCT-derived MD, MCSA, and pMRI-derived IMF as previously described[19], using 5% error as the benchmark for acceptable reproducibility. Pearson correlations described the relationship between MD and each of pMRI-derived absolute and percentage IMF. The relationship between single-slice IMF.A and 5-slice IMF.V was examined using a linear regression analysis.

A binary logistic regression analysis was performed to determine the relationship between pQCT-derived MD and fragility fractures in the last 14 years. The same model was performed for pQCT-derived MCSA, pMRI-derived IMF and total hip aBMD for comparison. These base models for muscle variables were examined with the addition of age, BMI and total hip aBMD as covariates in a second model. A third model added IMF into the second model that examined MD plus covariates. Predicted and observed outcomes were used to determine sensitivity and 1-specificity to construct receiver-operator characteristics (ROC) curves. Areas under the ROC curves (AUC) were reported along with binomial exact 95% confidence intervals. The AUCs for different models were compared using the method by Delong et al by measuring the generalized U-statistic[20]. All statistical analyses were performed on SAS v9.3 (SAS Institute Inc, Cary, NC, USA) and were evaluated at the 95% confidence level.

Results

A total of 71 women completed at least one set of baseline pMRI and pQCT imaging procedures, of whom 32(45.1%) had experienced at least one fragility fracture within the last 14 years. Of the 32 fractures, 10 were in the lower limb, 13 in the upper limb and 7 were in the axial skeleton. Women who have had a fracture were on average significantly older. Age-adjusted means for all variables between those with and without a history of fractures were not significantly different from one another. Muscle density was non-significantly smaller in those with a history of fragility fractures compared to those without (p=0.06) (Table 1). The inter-individual variation in total IMF.A and IMF.V was almost twice as large in the fractured group compared to the non-fractured group in non-age-adjusted means.

A difference in +1 mm^2 of IMF.A was associated with a corresponding +6.6 mm^3 difference in IMF.V with an unexplained error of 102 mm^3 (R^2=81.4%, p<0.001). Leg muscle IMF.A explained 50.1% of the variance in MD, and 53.9% after adjustment for BMI (p<0.001). A similar magnitude of the relationship was observed between IMF.V and MD (R^2=49.3%, with BMI: 50.6%). Only half as much variance in MD was explained by percentage IMF.A (20.6%) or IMF.V (28.4%) (p<0.001). Total hip aBMD was not correlated with any of leg MD, IMF.A, IMF.V or their corresponding percentage measures. Odds for fragility fractures

	No Fx (N=39)		≥1 Fx (N=32)		
	Means	**± SD**	**Mean**	**± SD**	**p-value**
Age (years)	**67.0**	**5.2**	**75.6**	**8.3**	**<0.01**
BMI (kg/m²)	27.06	0.96	28.56	1.06	0.25
TUG time (s)	10.2	0.3	10.1	0.3	0.87
Max grip strength (kg)	24.4	0.8	23.6	0.9	0.28
Duration of use (years):					
Antiresorptives	0.2	0.1	0.4	0.1	0.18
Calcium	6.8	1.4	7.5	1.6	0.76
Vitamin D_3	5.4	1.3	6.7	1.4	0.47
pQCT MD (mg/cm³)	70.37	0.62	69.17	0.69	0.06
pQCT MCSA (mm²)	5910	122	6243	135	0.12
pMRI IMF.A (mm²)	680	61	763	68	0.27
pMRI IMF.V (mm³)	3682	440	4327	487	0.16
pMRI Percent IMF.A (%)	15.6	1.3	16.0	1.5	0.99
pMRI Percent IMF.V (%)	16.6	1.9	17.7	2.2	0.59
Total hip aBMD (g/cm²)	0.869	0.020	0.871	0.022	0.79

Table 1. Comparison of participant characteristics between those with and without at least one fragility fracture. P-value indicates significant difference between groups from analysis of variance tests adjusted for multiple comparisons. Percent inter and intra-muscular fat (IMF) area (A) and volume (V) represent all visible muscle adiposity on T1-weighted MR images.

pMRI/pQCT Variable	OR (95% CI) Base Model	OR (95% CI) Adjusted	Per SD + / -
IMF.A	1.84 (0.95,3.57)	1.63 (0.60,4.44)	+377 mm²
IMF.V	**2.82 (1.19,6.70)**	1.95 (0.60,6.32)	+2837 mm³
%IMF.A + IMF.A	0.91 (0.56,1.49)	1.08(0.59,1.95)	+8.2%
%IMF.V + IMF.V	0.43 (0.14,1.31)	0.67 (0.24,1.91)	+11.8%
MD	**7.16 (2.17,23.42)**	4.69 (0.86,25.70)	-4.22 mg/cm³
MCSA	0.67 (0.40,1.12)	0.51 (0.19,1.33)	-766 mm²

Table 2a. Odds for fragility fractures associated with differences in MD and IMF variables. Binary logistic regression models computed odds for fragility fractures based on MD, IMF or percentage IMF. Base models are shown on the left column. Models adjusted by covariates (covars): age, BMI, total hip aBMD are shown on the right column. All odds ratios (OR) were expressed per standard deviation (SD) increase (+) or decrease (-) in the primary variable. All base models included all 71 participants (32 with fractures) and all adjusted models included 67 participants (30 with fractures).

pMRI/pQCT Variable	OR (95% CI) Base Model	OR (95% CI) Adjusted	Per SD + / -
MD + MCSA	**1.53 (0.78,2.97)**	1.28 (0.56,2.95)	-4.31 mg/cm³
MD + IMF.A	**11.27 (2.46,51.61)**	5.16 (0.78,34.12)	-4.22 mg/cm³
MD + IMF.V	**6.76 (1.61,27.65)**	4.29 (0.68,26.91)	-4.22 mg/cm³
MD + %IMF.A	**9.83 (2.61,36.76)**	5.45 (0.93,32.04)	-4.22 mg/cm³
MD + %IMF.V	**8.18 (2.36,28.40)**	5.08 (0.87,29.53)	-4.22 mg/cm³

Table 2b. Odds for fragility fractures associated with MD adjusted for IMF and covariates. Binary logistic regression models computed odds for fragility fractures based on MD as the variable of interest, and further adjusting for IMF variables. Base models are shown on the left column. Models adjusting for covariates (covars): age, BMI, total hip aBMD are shown on the right column. All odds ratios (OR) were expressed per standard deviation (SD) increase (+) or decrease (-) in the primary variable. All base models included all 71 participants (32 with fractures) and all adjusted models included 67 participants (30 with fractures).

Muscle variables	AUC	SE[a]	95% CI[b]	Comparison to AUC=0.50	Comparison to total hip aBMD
Total Hip aBMD	0.576	0.074	0.448 to 0.697	p=0.306	- -
pQCT MD	**0.782**	**0.058**	**0.663 to 0.874**	**p<0.001**	**p=0.047**
pQCT MCSA	0.586	0.068	0.453 to 0.719	p=0.219	P=0.620
pMRI IMF.A	0.627	0.075	0.499 to 0.743	p=0.080	p=0.685
pMRI IMF.V	**0.687**	**0.068**	**0.561 to 0.795**	**p=0.008**	p=0.342

Table 3. Comparison of areas under the ROC curves for muscle variables versus total hip aBMD on discriminative power for prevalent fragility fractures. Sensitivity and 1-specificity values were generated by estimates output from binary logistic regression analyses of IMF.A, IMF.V, MD and total hip aBMD on fragility fractures, plotted as receiver operator characteristics (ROC) curves for each variable alone. Areas under the ROC curves (AUC) were compared using the generalized U-statistic method by Delong et al.[20] against a null AUC of 0.50 and against the AUC determined for total hip aBMD. These analyses included all 71 women.

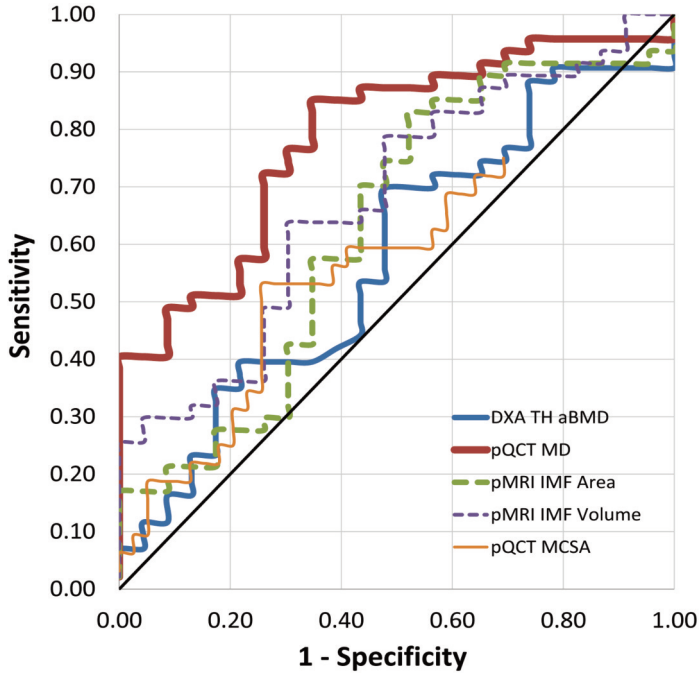

Figure 2. Comparison of ROC curves for muscle variables and total hip aBMD associations with prevalent fragility fractures. Receiver Operator Characteristics (ROC) curves analysis of the ability of pQCT-derived MD (thick/red line), MCSA (thin/orange line), DXA-derived total hip aBMD (medium/blue line), pMRI-derived IMF area (medium-dashed/green line) and IMF volume (thin-dashed/purple line) to discriminate between those with and without a history of fragility fractures. Black diagonal line represents reference cut off of 0.50 AUC. All 71 women were included in these analyses.

were significantly increased with lower MD and higher IMF.V alone but not with MCSA. Although a larger apparent odds for fractures was observed with larger IMF.A, this result was not significant (Table 2a). The association between MD and fragility fractures remained significant after adjusting for IMF.A or IMF.V (Table 2b) but was attenuated when MCSA, or age and BMI were included in the model and remained non-significant after including total hip aBMD. In post-hoc sensitivity analyses, age was shown to be a significant confounder to fractures (OR: 1.18 (1.08,1.28)), to MD ((R^2=0.254, B=-0.23 (-0.31, -0.15)), to MCSA ((R^2=0.106, B=-29.38(-46.44,-12.32)), and to IMF.V ((R^2=0.089, B=86.81 (30.80, 142.83)). Those with a history of lower limb fractures were non-significantly associated with longer TUG time after adjusting for age (OR: 1.13(0.54,2.37)). Age-adjusted relationships between MD and TUG time (R^2=0.41, B(-0.086(-0.204,0.031)) was also not significant.

Areas under the ROC curves were significantly larger than 0.50 for MD and IMF.V (Table 3) but only the discriminative power of MD for fractures was significantly larger than that of total hip aBMD (Figure 2). Discriminative power of MD

	All Participants N=51			No Fx and No Antiresorptives N=17		
Short-term Test-retest pMRI/pQCT Variable	**RMSCV**	**RMSSD**	**LSC**	**RMSCV**	**RMSSD**	**LSC**
MRI IMF.A (mm^2)	0.106	72	201	0.097	63	174
MRI IMF.V (mm^3)	0.061	261	724	0.053	180	499
pQCT MCSA (mm^2)	0.018	106	295	0.009	52	143
pQCT MD (mg/cm^3)	0.018	1.24	3.43	0.011	0.80	2.21
	N=33			**N=14**		
One-year Test-retest pMRI/pQCT Variable	**RMSCV**	**RMSSD**	**LSC**	**RMSCV**	**RMSSD**	**LSC**
MRI IMF.A (mm^2)	0.149	97	268	0.114	58	160
MRI IMF.V (mm^3)	0.171	823	2280	0.223	775	2149
pQCT MCSA (mm^2)	0.084	493	1367	0.042	252	699
pQCT MD (mg/cm^3)	0.026	1.77	4.91	0.021	1.45	4.02

Table 4. Short- and long-term precision error for test-retest analyses of muscle outcomes. Root mean square coefficients of variation (RMSCV), root mean square standard deviations (RMSSD) and least significant change (LSC) were computed for same day (top section) and one-year (bottom section) retesting of muscle measurements quantified from pMRI and pQCT images. Analyses were performed in all individuals (left) and in those who have not had a history of fragility fractures or were on antiresorptive therapy (right).

plus either IMF.V (AUC=0.796) or IMF.A (AUC=0.787) for fractures did not improve over MD alone (AUC=0.782) (graphs not shown). Combining MD with total hip aBMD yielded significantly larger AUC (0.798) compared to just total hip aBMD alone (AUC=0.576) ($p<0.001$) but not compared to just MD alone (AUC=0.782).

Both MD and MCSA derived from pQCT images were reproducible with RMSCV values under 5%. However, short-term test-retesting of both IMF.A and IMF.V exceeded the 5% benchmark (Table 4). Short-term but not long-term precision error was smaller for IMF.V compared to IMF.A. Examining only individuals without a history of fragility fractures or were not using antiresorptives resulted in a mild improvement in short- and long-term precision.

Discussion

Summary of results

In this study of 71 women (mean age: 72.8±8.4 years, mean BMI: 27.70±5.81 kg/m^2) with or without a history of fragility fractures, MD demonstrated the largest association with fragility fractures compared to other variables in base models. This inverse relationship remained significant and was strengthened, not abolished, by including pMRI-derived measures of IMF but was attenuated after accounting for age and total hip aBMD. In sensitivity analyses, age was shown to be a significant confounder to MD, MCSA, IMF volume and fractures. Muscle density was represented over 50% by IMF volume. Although IMF volume also exhibited a significant association with fractures, this association also did not hold after age adjustment and the discriminative power for fractures was not significantly larger than the null of 0.50 or that of total hip aBMD. All IMF measures exceeded the precision error benchmark of 5% whereas MD achieved a high degree of precision for both short- and long-term retesting.

Associations with fractures

The increased odds for fragility fractures associated with a -4.22 mg/cm^3 difference in MD can be interpreted as bone fragility related to fatty infiltration into muscle. The fact that larger amounts of IMF did associate with fractures further corroborates this proposition. However, addition of IMF into models containing MD did not attenuate the relationship seen between MD and fractures. Other unmeasured muscle factors should be explored to determine the component of MD that is in fact the primary correlate of fractures; for example, muscle fibre density, protein content or mitochondrial density. That these associations were attenuated after adjusting for age suggests that a large component of MD's relation to fractures may simply be an age-related effect. It is also possible that lower limb fractures resulted in more limited physical function, leading to lower muscle density; but sensitivity analyses only showed a non-significant association between fractures and TUG time. Moreover, physical function did not correlate significantly with MD after age adjustment.

In contrast to the lack of association between MCSA and fractures in the present study, Johannesdottir et al demonstrated a significant association between larger cross-sectional area of the total mid-thigh (hazard ratio: 0.5 (0.4-0.8) per SD increase) and a lower risk of incident lower extremity fragility

fractures in a study of men (N=1838) and women (N=1924) 66 to 96 years of age[21]. Although they also saw an effect for higher knee extensor strength (HR: 0.6 (0.5-0.9)), the investigators did not quantify MD. Schafer et al showed that in 2762 men and women of the Health Aging and Body Composition (ABC) study, lower MD of the thigh was associated with an increased risk for incident fragility fractures (HR: 1.19 (1.04-1.36) independent of glucose metabolism status (p=0.65 for interaction)[15]. This study suggests that fracture risk-associated muscle fat infiltration may not be restricted to diabetics. While fat invasion of muscle may be related to aging, one study showed that poorer muscle strength was associated with an increased risk of fractures during aerobic activities, even at a young age[22]. Supporting the association between IMF and fractures observed in this study, Sheu et al. also saw that direct measurements of intermuscular adipose tissue from QCT scans of the abdomen were linked to incident non-vertebral fractures[14].

Discriminative power for individuals with a history of fragility fractures

The AUC for prevalent fragility fractures observed here for total hip aBMD was smaller (0.58) than previously reported non-spine (0.65) and spinal incident fractures (0.68)[23] in 4124 women of the Study of Osteoporotic Fractures. Majumdar (0.73)[24] and Frost (0.80)[25] et al also showed larger AUCs for total hip aBMD than reported here. Despite these vast differences in AUCs across studies, there remained a sizeable difference in AUCs between aBMD and MD derived from pQCT images in the present study. As a point of comparison, distal radius trabecular number in Majumdar's study (0.69 vs. 0.73 for total hip aBMD) and broadband ultrasound attenuation (0.77-0.83 vs. 0.80 for total hip aBMD) in Frost's study generated AUCs for prevalent fractures that were either smaller or comparable to total hip aBMD. The discriminative power of muscle variables on individuals with a history of fragility fractures has not previously been demonstrated.

Validity and precision of muscle outcomes

The ability of MD to act as a proxy for muscle adiposity was first validated here *in vivo* using 1.0T pMRI-derived IMF measurements. The large percentage of variance in MD explained by IMF (approximately 50%) supports the proposal that MD could serve as an estimate of IMF. In fact, it may be a feasible alternative especially as the precision error of MD is substantially smaller than IMF. The reproducibility of IMF measurements is challenged by the subjectivity imposed when selecting the lower threshold for separating fat from muscle signals. However, by examining a larger volume, the short-term retest error was reduced. In spite of the advantage of examining a volume, single slice IMF area still correlated to a high degree to IMF volume. Cotofana et al also demonstrated a similar finding in the thigh muscles[26]. Beattie et al segmented intermuscular fat in quadriceps muscles in one study, yielding also an RMSCV just above 5% for re-analysis precision[27]. Until more standardized segmentation approaches are developed, the precision of IMF outcomes may remain less desirable than MD. On the flip side of the MD measurement, the remaining unaccounted variance could reflect other properties of muscle as muscle fibre density, protein content or mitochondrial density. The MRI sequence utilized in the present study cannot enable the quantification of muscle fibre information. However, with diffusion tensor imaging, it may be possible to gain an appreciation of the quality of muscle fibres[28].

Study limitations

The smaller sample size observed in this study may have limited the statistical power for obtaining more precise effect sizes for both odds ratios and AUCs for fragility fractures, particularly in models that adjusted for age. Total hip aBMD values were obtained within one to three years of muscle measurements. Although one year changes in aBMD (-0.53%, in N=6007 Caucasian women mean age 73 years) are not considered to be substantial[29], three year changes (projected -1.59%) could differentially impact fracture risk. The prevalent fractures were also obtained retrospectively. In this cross-sectional analysis, the direction of causality was difficult to establish. It is possible that the differences in muscle measurements observed between individuals were the result of reduced mobility post-fracture. However, in sensitivity analyses, the association between lower limb fractures and 'up-and-go' time was not significant. A prospective study focused on incident fractures as the primary outcome would be necessary to confirm the results observed here. The challenge of measuring inter- and intra-muscular fat directly lies in the lack of pMRI modalities available to execute a study large enough to address the 1.72% annual incidence of fractures[30]. The pMRI scans obtained at the leg were limited to fast spin echo sequences. The signal of the resultant images reflects a combination of both water and fat proton signals. Although it is not expected that apparent streaks of fat within muscle contain a significant amount of water, superior fat imaging sequences including the "iterative decomposition of water and fat with echo asymmetry and least squares estimation" (IDEAL) method are available on full-body MRI systems to achieve this goal. Currently, the 1.0T pMRI modality does not enable this more advanced sequence to be performed. The present study also did not separate inter- from intra-muscular fat deposits. It is expected that this procedure will introduce greater subjectivity and result in poorer test-retest precision than demonstrated here. With refinement of the technique for separating these fat compartments, it would be beneficial to understand how inter and intra-muscular fat differentially affect the risk for a fragility fracture.

Conclusions

Having larger amounts of inter- and intra-muscular fat at the leg was not shown to be a significant risk factor for fractures here after adjusting for age. The present study was underpowered to observe the effect sizes reported here with sufficient precision. In addition, the cross-sectional nature of

the study data prevents conclusions regarding the direction of causality of the muscle density and fractures association. Muscle density derived from pQCT images of the leg was shown to be a valid proxy for inter- and intra-muscular fat *in vivo*. Although MRI-derived inter- and intra-muscular fat volume demonstrated an association with prevalent fractures before age adjustment, the measurement remained limited by poorer retesting precision. Muscle density is a reliable alternative for estimating the amount of fat within muscle, but larger studies examining fractures prospectively are required to better conclude on how it may be a potential risk factor for fractures.

References

1. Hughes JM, Petit MA. Biological underpinnings of Frost's mechanostat thresholds: the important role of osteocytes. J Musculoskelet Neuronal Interact 2010; 10:128-35.
2. Macdonald HM, Kontulainen SA, Mackelvie-O'Brien KJ, Petit MA, Janssen P, Khan KM, McKay HA. Maturity- and sex-related changes in tibial bone geometry, strength and bone-muscle strength indices during growth: a 20-month pQCT study. Bone 2005;36:1003-11.
3. Rantalainen T, Heinonen A, Komi PV, Linnamo V. Neuromuscular performance and bone structural characteristics in young healthy men and women. Eur J Appl Physiol 2008;102:215-22.
4. Wong AK, Cawthon PM, Peters KW, Cummings SR, Gordon CL, Sheu Y, Ensrud K, Petit M, Zmuda JM, Orwoll E, Cauley J, Osteoporotic Fractures in Men Research G. Bone-muscle indices as risk factors for fractures in men: the Osteoporotic Fractures in Men (MrOS) Study. J Musculoskelet Neuronal Interact 2014;14:246-54.
5. Pino AM, Rosen CJ, Rodriguez JP. In osteoporosis, differentiation of mesenchymal stem cells (MSCs) improves bone marrow adipogenesis. Biol Res 2012;45:279-87.
6. Savopoulos C, Dokos C, Kaiafa G, Hatzitolios A. Adipogenesis and osteoblastogenesis: trans-differentiation in the pathophysiology of bone disorders. Hippokratia 2011;15:18-21.
7. Zhang H, Lu W, Zhao Y, Rong P, Cao R, Gu W, Xiao J, Miao D, Lappe J, Recker R, Xiao GG. Adipocytes derived from human bone marrow mesenchymal stem cells exert inhibitory effects on osteoblastogenesis. Curr Mol Med 2011;11:489-502.
8. Syed FA, Iqbal J, Peng Y, Sun L, Zaidi M. Clinical, cellular and molecular phenotypes of aging bone. Interdiscip Top Gerontol 2010;37:175-92.
9. Goodpaster BH, Kelley DE, Thaete FL, He J, Ross R. Skeletal muscle attenuation determined by computed tomography is associated with skeletal muscle lipid content. J Appl Physiol 2000;89:104-10.
10. McDermott MM, Ferrucci L, Guralnik J, Tian L, Liu K, Hoff F, Liao Y, Criqui MH. Pathophysiological changes in calf muscle predict mobility loss at 2-year follow-up in men and women with peripheral arterial disease. Circulation 2009;120:1048-55.
11. LaRoche DP, Cremin KA, Greenleaf B, Croce RV. Rapid torque development in older female fallers and nonfallers: a comparison across lower-extremity muscles. J Electromyogr Kinesiol 2010;20:482-8.
12. Tinetti ME. Clinical practice. Preventing falls in elderly persons. N Engl J Med 2003;348:42-9.
13. Ruan XY, Gallagher D, Harris T, Albu J, Heymsfield S, Kuznia P, Heshka S. Estimating whole body intermuscular adipose tissue from single cross-sectional magnetic resonance images. J Appl Physiol 2007;102:748-54.
14. Sheu Y, Marshall LM, Holton KF, Caserotti P, Boudreau RM, Strotmeyer ES, Cawthon PM, Cauley JA. Abdominal body composition measured by quantitative computed tomography and risk of non-spine fractures: the Osteoporotic Fractures in Men (MrOS) Study. Osteoporos Int 2013;24:2231-41.
15. Schafer AL, Vittinghoff E, Lang TF, Sellmeyer DE, Harris TB, Kanaya AM, Strotmeyer ES, Cawthon PM, Cummings SR, Tylavsky FA, Scherzinger AL, Schwartz AV, Health A, Body Composition S. Fat infiltration of muscle, diabetes, and clinical fracture risk in older adults. J Clin Endocrinol Metab 2010;95:E368-72.
16. Kreiger N, Tenenhouse A, Joseph L, MacKenzie T, Poliquin S, Brown JP, Prior JC, Rittmaster RS. Research notes: The Canadian Multicentre Osteoporosis Study (CaMos) - background, rationale, methods. Can J Aging 1999;18:12.
17. Podsiadlo D, Richardson S. The timed "Up & Go": a test of basic functional mobility for frail elderly persons. J Am Geriatr Soc 1991;39:142-8.
18. Guerra RS, Amaral TF. Comparison of hand dynamometers in elderly people. J Nutr Health Aging 2009;13:907-12.
19. Gluer CC, Blake G, Lu Y, Blunt BA, Jergas M, Genant HK. Accurate assessment of precision errors: how to measure the reproducibility of bone densitometry techniques. Osteoporos Int 1995;5:262-70.
20. DeLong ER, DeLong DM, Clarke-Pearson DL. Comparing the areas under two or more correlated receiver operating characteristic curves: a nonparametric approach. Biometrics 1988;44:837-45.
21. Johannesdottir F, Aspelund T, Siggeirsdottir K, Jonsson BY, Mogensen B, Sigurdsson S, Harris TB, Gudnason VG, Lang TF, Sigurdsson G. Mid-thigh cortical bone structural parameters, muscle mass and strength, and association with lower limb fractures in older men and women (AGES-Reykjavik Study). Calcif Tissue Int 2012;90:354-64.
22. Clark EM, Tobias JH, Murray L, Boreham C. Children with low muscle strength are at an increased risk of fracture with exposure to exercise. J Musculoskelet Neuronal Interact 2011;11:196-202.
23. Hillier TA, Stone KL, Bauer DC, Rizzo JH, Pedula KL, Cauley JA, Ensrud KE, Hochberg MC, Cummings SR. Evaluating the value of repeat bone mineral density meas-

urement and prediction of fractures in older women: the study of osteoporotic fractures. Arch Intern Med 2007; 167:155-60.
24. Majumdar S, Link TM, Augat P, Lin JC, Newitt D, Lane NE, Genant HK. Trabecular bone architecture in the distal radius using magnetic resonance imaging in subjects with fractures of the proximal femur. Magnetic Resonance Science Center and Osteoporosis and Arthritis Research Group. Osteoporos Int 1999;10:231-9.
25. Frost ML, Blake GM, Fogelman I. Does quantitative ultrasound imaging enhance precision and discrimination? Osteoporos Int 2000;11:425-33.
26. Cotofana S, Hudelmaier M, Wirth W, Himmer M, Ring-Dimitriou S, Sanger AM, Eckstein F. Correlation between single-slice muscle anatomical cross-sectional area and muscle volume in thigh extensors, flexors and adductors of perimenopausal women. Eur J Appl Physiol 2010;110:91-7.
27. Beattie KA, MacIntyre NJ, Ramadan K, Inglis D, Maly MR. Longitudinal changes in intermuscular fat volume and quadriceps muscle volume in the thighs of women with knee osteoarthritis. Arthritis Care Res (Hoboken) 2012;64:22-9.
28. Okamoto Y, Okamoto T, Yuka K, Hirano Y, Isobe T, Minami M. Correlation between pennation angle and image quality of skeletal muscle fibre tractography using deterministic diffusion tensor imaging. J Med Imaging Radiat Oncol 2012;56:622-7.
29. Cauley JA, Lui LY, Stone KL, Hillier TA, Zmuda JM, Hochberg M, Beck TJ, Ensrud KE. Longitudinal study of changes in hip bone mineral density in Caucasian and African-American women. J Am Geriatr Soc 2005; 53:183-9.
30. Langsetmo L, Hanley DA, Kreiger N, Jamal SA, Prior J, Adachi JD, Davison KS, Kovacs C, Anastassiades T, Tenenhouse A, Goltzman D. Geographic variation of bone mineral density and selected risk factors for prediction of incident fracture among Canadians 50 and older. Bone 2008;43:672-8.